JNeurosci THE JOURNAL OF NEUROSCIENCE

Research Articles: Neurobiology of Disease

Inhibition of IL-1β signaling normalizes NMDA-dependent neurotransmission and reduces seizure susceptibility in a mouse model of Creutzfeldt-Jakob disease

Ilaria Bertani[1], Valentina Iori[1], Massimo Trusel[2], Mattia Maroso[1], Claudia Foray[1], Susanna Mantovani[1], Raffaella Tonini[2], Annamaria Vezzani[1] and Roberto Chiesa[1]

[1]*Department of Neuroscience, IRCCS – Istituto di Ricerche Farmacologiche Mario Negri, 20156 Milan, Italy*
[2]*Neuroscience and Brain Technologies Department, Istituto Italiano di Tecnologia, 16163 Genoa, Italy*

DOI: 10.1523/JNEUROSCI.1301-17.2017

Received: 5 May 2017

Revised: 31 July 2017

Accepted: 23 August 2017

Published: 18 September 2017

Author contributions: I.B., V.I., M.T., M.M., C.F., and S.M. performed research; I.B., V.I., M.T., M.M., C.F., R.T., A.V., and R.C. analyzed data; R.T., A.V., and R.C. designed research; A.V. and R.C. wrote the paper.

Conflict of Interest: The authors declare no competing financial interests.

This work was supported by grants from Telethon-Italy (GGP12115), Fondazione Cariplo (2012-0560), the Italian Ministry of Health (RF-2010-2314035), the European Union's Seventh Framework Programme (FP7/2007-2013) under grant agreement no. 602102 (EPITARGET), and from the Fondazione Istituto Italiano di Tecnologia.

Correspondence should be addressed to Roberto Chiesa, Department of Neuroscience, IRCCS — Istituto di Ricerche Farmacologiche Mario Negri, Via G. La Masa 19, 20156 Milan, Italy.E-mail: roberto.chiesa@marionegri.it

Cite as: J. Neurosci ; 10.1523/JNEUROSCI.1301-17.2017

Inhibition of IL-1β signaling normalizes NMDA-dependent neurotransmission and reduces seizure susceptibility in a mouse model of Creutzfeldt-Jakob disease

Ilaria Bertani[1,*], Valentina Iori[1,*], Massimo Trusel[2,*], Mattia Maroso[1], Claudia Foray[1], Susanna Mantovani[1], Raffaella Tonini[2], Annamaria Vezzani[1], and Roberto Chiesa[1]

[1]Department of Neuroscience, IRCCS – Istituto di Ricerche Farmacologiche Mario Negri, 20156 Milan, Italy
[2]Neuroscience and Brain Technologies Department, Istituto Italiano di Tecnologia, 16163 Genoa, Italy

*These authors contributed equally to this work

Correspondence should be addressed to Roberto Chiesa, Department of Neuroscience, IRCCS – Istituto di Ricerche Farmacologiche Mario Negri, Via G. La Masa 19, 20156 Milan, Italy.E-mail: roberto.chiesa@marionegri.it

Abbreviated title: IL-1β alters glutamatergic transmission in CJD mice
Number of pages: 24
Number of figures: 6
Number of words: 240 (Abstract), 594 (Introduction), and 1,531 (Discussion)
Conflict of interests: The authors declare no competing financial interests.
Acknowledgments: This work was supported by grants from Telethon-Italy (GGP12115), Fondazione Cariplo (2012-0560), the Italian Ministry of Health (RF-2010-2314035), the European Union's Seventh Framework Programme (FP7/2007-2013) under grant agreement no. 602102 (EPITARGET), and from the Fondazione Istituto Italiano di Tecnologia.

Abstract

Creutzfeldt-Jakob disease (CJD) is a neurodegenerative disorder caused by prion protein (PrP) misfolding, clinically recognized by cognitive and motor deficits, electroencephalographic (EEG) abnormalities and seizures. Its neurophysiological bases are not known. To assess the potential involvement of *N*-methyl-D-aspartate receptor (NMDAR) dysfunction, we analyzed NMDA-dependent synaptic plasticity in hippocampal slices from Tg(CJD) mice, which model a genetic form of CJD. Because PrP depletion may result in functional upregulation of NMDARs, we also analyzed PrP knockout (KO) mice. Long-term potentiation (LTP) at the Schaffer collateral-commissural synapses in the CA1 area of ~100-day-old Tg(CJD) mice was comparable to that of wild-type (WT) controls, but there was an inversion of metaplasticity, with increased GluN2B phosphorylation, indicative of enhanced NMDAR activation. Similar but less marked changes were seen in PrP KO mice. At ~300 days of age, the magnitude of LTP increased in Tg(CJD), but decreased in PrP KO mice, indicating divergent changes in hippocampal synaptic responsiveness. Tg(CJD) but not PrP KO mice were intrinsically more susceptible than WT controls to focal hippocampal seizures induced by kainic acid. IL-1β-positive astrocytes increased in the Tg(CJD) hippocampus, and blocking IL-1 receptor signaling restored normal synaptic responses and reduced seizure susceptibility. These results indicate that alterations in NMDA-dependent glutamatergic transmission in Tg(CJD) mice do not depend solely on PrP functional loss. Moreover, astrocytic IL-1β plays a role in the enhanced synaptic responsiveness and seizure susceptibility, suggesting that targeting IL-1β signaling may offer a novel symptomatic treatment for CJD.

Significance statement

Individuals with Creutzfeldt-Jakob disease (CJD), an incurable brain disorder caused by alterations in prion protein structure, develop dementia and myoclonic jerks; they are prone to seizures, and have high brain levels of the inflammatory cytokine IL-1β. Here we show that blocking IL-1β receptors with anakinra, the human recombinant form of the endogenous IL-1 receptor antagonist used to treat rheumatoid arthritis, normalizes hippocampal neurotransmission and reduces seizure susceptibility in a CJD mouse model. These results link neuroinflammation to defective neurotransmission and the enhanced susceptibility to seizures in CJD, and raise the possibility that targeting IL-1β with clinically available drugs may be beneficial for symptomatic treatment of the disease.

Introduction

Prion diseases are invariably fatal neurodegenerative disorders of humans and other mammals caused by misfolding of the cellular prion protein (PrP^{C}), a cell surface glycoprotein of uncertain function (Chiesa, 2015). Creutzfeldt-Jakob disease (CJD) is the most common form in humans. It can arise sporadically, be dominantly inherited due to mutations in the *PRNP* gene encoding PrP^{C}, or acquired by contact with exogenous PrP^{Sc}, the infectious PrP isoform (prion) which propagates by inducing misfolding of host-encoded PrP^{C} (Colby and Prusiner, 2011; Head and Ironside, 2012).

CJD has a stereotyped clinical course. Altered mental function is the initial manifestation, including dementia, confusion, disorientation, behavior abnormalities and depression of other higher cortical functions. Later, myoclonic jerks, rigidity, and extrapyramidal and cerebellar abnormalities become prominent.

In about two-thirds of patients, electroencephalography (EEG) detects typical periodic sharp wave complexes (PSWCs), either lateralized or generalized (Wieser et al., 2006). Epileptiform discharges and focal motor or generalized seizures may also be observed, typically in the late stage of the disease (Wieser et al., 2006). Nonconvulsive status epilepticus is sometimes a presenting symptom in CJD (Espinosa et al., 2010). This suggests that changes in neuronal network excitability occur in seizure-prone brain areas. As the patients near death, they become akinetic, unresponsive, mute and rigid (Head and Ironside, 2012; Puoti et al., 2012).

The pathogenic mechanisms responsible for this complex symptomatology are not known. Studies in animal models have suggested several toxic mechanisms activated by abnormally folded PrP that may lead to neuronal dysfunction and death, including corruption of *N*-methyl-D-aspartate receptor (NMDAR) activity (Chiesa, 2015). Increased NMDAR-dependent excitation has been reported in mice inoculated with variant (v) CJD prions (Ratte et al., 2008), and when PrP^{Sc}, or the PrP^{Sc}-like PrP106-126 peptide, was exogenously presented to cultured neurons, NMDAR antagonists blocked the resulting neurotoxicity (Muller et al., 1993; Perovic et al., 1995; Brown et al., 1997; Resenberger et al., 2011; Thellung et al., 2012).

Loss of a physiological PrP^{C} function in regulating NMDAR activity may also contribute to the pathogenic process. Genetic PrP^{C} depletion results in increased hippocampal NMDAR-mediated excitation and glutamate exicitotoxicity (Khosravani et al., 2008). In addition, PrP knockout (KO) mice are reported to be more susceptible to seizures induced by kainic acid (KA) than wild-type (WT) controls (Walz et al., 1999; Rangel et al., 2007), perhaps because of facilitated NMDAR-mediated excitation in the hippocampus (Maglio et al., 2004; Rangel et al., 2009); although this issue remains controversial (Striebel et al., 2013b; Carulla et al., 2015).

Deposition of misfolded/aggregated PrP and astro- and micro-gliosis are typical neuropathological changes in CJD (Sikorska et al., 2012). In addition, CJD brains have high levels of several inflammatory cytokines, including IL-1β (Sharief et al., 1999; Shi et al., 2013; Llorens et al., 2014). However, it is not clear which cell population is responsible for the increase in IL-1β, and whether this proinflammatory cytokine contributes to enhancing NMDAR-mediated glutamatergic transmission (Viviani et al., 2003; Balosso et al., 2008), lowering the threshold for seizures (Vezzani and Viviani, 2015).

We previously generated Tg(CJD) mice expressing the mouse (mo) PrP homolog of the D178N/V129 mutation linked to genetic CJD (Dossena et al., 2008). These mice synthesize a misfolded form of mutant PrP in their brains, and develop clinical and neuropathological features highly reminiscent of CJD, including memory and motor deficits, abnormal EEG patterns mimicking the human PSWCs, PrP deposition and gliosis (Dossena et al., 2008).

The present study provides evidence of dysfunctional NMDA-dependent hippocampal synaptic plasticity and enhanced seizure susceptibility in Tg(CJD) mice, resulting from a combination of loss and gain of function of mutant PrP, exacerbated by neuroinflammation.

Materials and Methods

Experimental design and statistical analysis. All animal experiments were designed in accordance with the ARRIVE (Animal Research: Reporting of In Vivo Experiments) guidelines (Kilkenny et al., 2010), with a commitment to refinement, reduction, and replacement, minimizing the numbers of mice, while using biostatistics to optimize mouse numbers [as used in our previously published peer-reviewed work (Nazzaro et al., 2012; Bouybayoune et al., 2015; Trusel et al., 2015; Iori et al., 2017)]. Thus, for statistical validity, we used 5-10 mice for electrophysiology, 6-10 for analysis of KA-induced seizures, and 4-10 for reverse transcription quantitative real-time PCR (RT-qPCR), biochemical analysis and histology (the number of mice used in each experiment is reported in the figure legends). No sex-related differences in the Tg(CJD) phenotype were observed, so both male and female mice were used for RT-qPCR, biochemistry and histology. Males were used for electrophysiology and analysis of hippocampal seizures, to avoid variations due to ovarian cycles in females (Mejías-Aponte et al., 2002; Twele et al., 2016). Simple randomization was used for treatment allocation. Blinding was applied to treatment administration and data analysis.

For each variable, differences between the groups were assessed using independent samples Student's t test, one-way analysis of variance (ANOVA), two-way ANOVA (genotype and/or drug treatment as independent factors) followed by Tukey's, Mann-Whitney or Holm-Sidak's post hoc analysis when appropriate (details are reported in the figure legends). Synaptic plasticity data were analyzed with one-way ANOVA for repeated measures (RM1W) or two-way ANOVA for repeated measures (RM2W) followed by Tukey's post hoc analysis; n indicates number of recordings.

Mice. Production of Tg(CJD) mice, expressing moPrP D177N/V128 tagged with an epitope for monoclonal antibody 3F4 has already been reported (Dossena et al., 2008). We used mice of the Tg(CJD-A21$^{+/-}$)/*Prnp*$^{0/0}$ line expressing 3F4-tagged D177N/V128 PrP at ~1X, that had been backcrossed for more than ten generations with an inbred colony of Zürich I *Prnp*$^{0/0}$ mice (Bueler et al., 1992) with a pure C57BL/6J background (C57BL/6J/*Prnp*$^{0/0}$; European Mouse Mutant Archive, Monterotondo, Rome, Italy; RRID:IMSR_EM:01723). The status of the transgene was determined by PCR (Dossena et al., 2008). PrP KO mice were nontransgenic littermates of Tg(CJD-A21$^{+/-}$)/*Prnp*$^{0/0}$ mice. Age-matched C57BL/6J (WT) mice were purchased from Envigo (http://www.envigo.com/products-services/research-models-services/models/research-models/mice/inbred/c57bl-6-inbred-mice/c57bl-6jrcchsd/). Mice were housed at constant room temperature (23°C) and relative humidity (60 ± 5%) with free access to food and water and a fixed 12-h light/dark cycle. To reduce experimental variability due to different husbandry conditions, WT mice purchased from Envigo were housed in the same animal room as Tg(CJD) and PrP KO mice for from at least two weeks to several months.

Procedures involving animals and their care were conducted in conformity with the institutional guidelines at the IRCCS – Mario Negri Institute for Pharmacological Research in compliance with national (D.lgs 26/2014; Authorization no. 19/2008-A issued March 6, 2008 by Ministry of Health) and international laws and policies (EEC Council Directive 2010/63/UE; the NIH Guide for the Care and Use of Laboratory Animals, 2011 edition). They were reviewed and approved by the Mario Negri Institute Animal Care and Use Committee, which includes ad hoc members for ethical issues, and by the Italian Ministry of Health (Decreto no. 62/2012-B and 212/2016-PR). Animal facilities meet international standards and are regularly checked by a certified veterinarian who is responsible for health monitoring, animal welfare supervision, experimental protocols and review of procedures.

Determination of NMDARs on post-synaptic density (PSD). Subcellular fractionation of the mouse hippocampus was as described (Balducci et al., 2010). Tissue was homogenized in ice-cold 0.32 M sucrose containing 1 mM Hepes, 1mM $MgCl_2$, 1 mM $NaHCO_3$, 0.1 mM, PMSF, at pH 7.4, with a complete set of protease inhibitors (SigmaFast, Sigma-Aldrich) and phosphatase inhibitors (PhosSTOP, Roche Life Science).

The homogenized tissue was centrifuged at 1,000 x g for 5 min and the supernatant was centrifuged at 13,000 x g for 15 min to obtain a crude membrane fraction. The pellet was then resuspended in 1 mM Hepes containing protease and phosphatase inhibitors, and centrifuged at 100,000 x g for 1 h. The resulting pellet was resuspended in a buffer containing 75 mM KCl, protease and phosphatase inhibitors and 1% Triton-X 100 and centrifuged at 100,000 x g for 1h. The final pellet was homogenized in a glass-glass Potter homogenizer in 20 mM Hepes with protease and phosphatase inhibitors; this fraction, referred to as the Triton-insoluble fraction (TIF), was stored at -80°C. The protein composition of this preparation was tested for the absence of the presynaptic marker synaptophysin and enrichment in PSD proteins. Proteins (10 μg) were resolved by sodium dodecyl sulfate polyacrylamide gel electrophoresis (SDS-PAGE) and electrophoretically transferred to poly-vinylidene fluoride (PVDF) membranes. The membranes were blocked for 1 h in 5% non-fat dry milk in Tris-buffered saline 0.1 M, pH 7.4, containing 0.01% Tween 20 (TTBS), then incubated with the primary antibody diluted in blocking solution, with the exception of anti-phospho-Tyr1472 GluN2B, which was diluted in TTBS containing 5% bovine serum albumin (BSA). The antibodies were: mouse monoclonal anti-GluN1 (1:1,000; Synaptic System RRID:AB_2113443), rabbit polyclonal anti-phospho-Tyr1472 GluN2B (1:700; Thermo Scientific RRID: AB_325370), rabbit polyclonal anti-GluN2A (1:2,000; Molecular Probes RRID:AB_2536209), anti-GluN2B (1:2,000; Molecular Probes RRID:AB_2536210), mouse monoclonal anti-PSD95 (1:10,000; NeuroMab RRID:AB_10698024), mouse monoclonal anti-β-actin (1:20,000; Millipore RRID:AB_2223041). After thorough rinsing in TTBS, the blots were incubated with horseradish peroxidase-conjugated secondary antibodies, revealed using enhanced chemiluminescence (Luminata Forte, Millipore) and visualized by a Biorad XRS image scanner. Quantity-One software (Bio-Rad) was used for quantitative densitometry of protein bands.

Histology. Mice were deeply anesthetized by intraperitoneal injection of 100 mg/kg ketamine hydrochloride and 1 mg/kg medetomidine hydrochloride (Alcyon), and perfused through the ascending aorta with phosphate buffered saline (PBS 0.05 M; pH 7.4) followed by 4% paraformaldehyde (PFA) in PBS. Brains were removed, post-fixed, cryoprotected and frozen at -80°C. Sections were cut throughout the septo-temporal aspects of the hippocampus using a Leica cryostat and incubated for 1 h at RT with 10% normal goat serum (NGS), 1% Triton X-100 in TBS 0.1 M, pH 7.4, then overnight at 4°C with rabbit polyclonal anti-GFAP antibody (Dako; 1:2,500 RRID:AB_10013382), rat polyclonal anti-CD11b (Serotec; 1:1,000 RRID:AB_321292), goat polyclonal anti-IL-1β (Santa Cruz; 1:200 RRID:AB_2124627), followed by visualization with the Vectastain ABC kit (Vector), with 3,3' diaminobenzidine (DAB) (or nickel-intensified DAB for IL-1β) as chromogen. The TSA Cyanine 5 System (Perkin Elmer) was used for immunoflorescent staining of IL-1β. Anti-rat (RRID:AB_141709) and anti-rabbit IgG Alexa 488 (RRID:AB_143165) (1:500, Molecular Probes) were used for immunoflorescent staining of CD11b and GFAP, respectively. Sections were reacted with 2 μg/mL Hoechst 33258 (Molecular probes RRID:AB_2651133) to stain the nuclei. Slices were matched at comparable antero-posterior and dorso-ventral levels for comparison of the different experimental groups.

Reverse transcription quantitative real-time PCR (RT-qPCR). Total RNA from the mouse hippocampus was extracted using the SV Total *RNA* Isolation System (Promega) according to the manufacturer's instructions; 1-2 μg of RNA was reverse transcribed with the High-Capacity cDNA Kit (Life Technologies) and cDNA amplified by a 7900 HT Sequence Detection System (Life Technologies). Samples were always processed in triplicate. The relative gene expression was calculated by the formula $2^{(-\Delta\Delta Ct)}$ using a defined group as reference ($2^{(-\Delta\Delta Ct)} = 1$). The primer sequences were: 5'-CTCCATGAGCTTTGTACAAGG-3' for IL-1β forward and 5'-TGCTGATGTACCAGTTGGGG-3' for IL-1β reverse; 5'-AGGTCGGTGTGAACGGATTTG-3' for GAPDH forward and 5'-TGTAGACCATGTAGTAGTTGAGGTCA-3' for GAPDH reverse (De Simoni et al., 2000).

Electrophysiology. Male mice were anesthetized with isofluorane and decapitated, and their brains were transferred to ice-cold dissecting artificial cerebrospinal fluid (aCSF) containing 87 mM NaCl, 75 mM sucrose, 2.5 mM KCl, 1.25 mM NaH_2PO_4, 7 mM $MgCl_2$, 0.5 mM $CaCl_2$, 25 mM $NaHCO_3$ and 25 mM D-glucose, saturated with 95% O_2 and 5% CO_2 (Bischofberger et al., 2006). Oblique coronal sections (350 μm thick) were cut using a Vibratome 1000S slicer (Leica), then transferred to aCSF containing 115 mM NaCl, 3.5 mM KCl, 1.2 mM NaH_2PO_4, 1.3 mM $MgCl_2$, 2 mM $CaCl_2$, 25 mM $NaHCO_3$, and 25 mM D-glucose and aerated with 95% O_2 and 5% CO_2. After 15 min at 32°C, slices were kept at 22-24°C. During experiments, slices were continuously superfused with aCSF at a rate of 2 mL/min at 28°C.

Extracellular recordings of field postsynaptic potentials (fPSP) were obtained in the CA1 stratum radiatum, using glass micropipettes filled with aCSF. Stimuli (50-160 μA, 50 μs) to excite Shaffer collaterals were delivered through a bipolar twisted tungsten electrode placed 400 μm from the recording electrode. LTP was induced using the following theta burst stimulation protocol (TBS): 10 trains (4 pulses at 100 Hz) at 5 Hz, repeated twice with a 2-min interval. To induce metaplasticity, we applied a priming low-frequency stimulation protocol (LFS, 10-Hz, 10 pulses repeated twice, separated by 1 second) delivered 25 min before TBS (Costello et al., 2012). The magnitude of synaptic plasticity was evaluated by comparing the fPSP normalized slopes from the last 5 min of baseline recordings with those 18-26 min after LFS or 35-45 min after TBS planned comparison.

Mouse model of seizures. Male mice (6-10) were surgically implanted under general gas anesthesia (1-3% isoflurane in O_2) and stereotaxic guidance (Iori et al., 2013). Two nichrome-insulated bipolar depth electrodes (60 μm OD) were implanted bilaterally into the dorsal hippocampus (from bregma, mm: nose bar 0; anteroposterior –1.8, lateral 1.5 and 2.0 below dura mater). A 23-gauge cannula was unilaterally positioned on top of the *dura mater* and glued to one of the depth electrodes for the intrahippocampal injection of KA (Balosso et al., 2008; Iori et al., 2013, 2017). The electrodes were connected to a multipin socket and, together with the injection cannula, were secured to the skull with acrylic dental cement. KA (Sigma-Aldrich, Saint Louis, MO, USA) was injected intrahippocampally in freely moving mice, seven days after surgery (Iori et al., 2013). KA 7 ng in 0.5 μL was dissolved in 0.1 M PBS, pH 7.4, and injected unilaterally in the dorsal hippocampus in freely moving mice using a needle protruding 2.0 mm from the bottom of the guide cannula. The needle was left in place for one more minute to avoid backflow through the cannula. This dose of KA induces EEG ictal episodes in the hippocampus in 100% of mice with no mortality (Iori et al., 2013). Human recombinant IL-1 receptor antagonist (anakinra) (Biovitrum AB, Stockolm, Sweden) was diluted in sterile saline and bilaterally injected intracerebroventricularly (0.5 μg/0.5 μl/side) in mice, 10 min before KA. For injection of saline or anakinra, mice were implanted with two additional cannulae bilaterally on top of the *dura mater*.

EEG activity was recorded using the Twin EEG Recording System (version 4.5.3.23) connected with a Comet AS-40 32/8 Amplifier (sampling rate 400 Hz, high-pass filter 0.3 Hz, low-pass filter 70 Hz, sensitivity 2000 mV/cm; Grass-Telefactor, West Warwick, R.I., USA). Digitized EEG data were processed using the Twin record and review software. EEG was recorded for 30 min before KA injection to assess baseline activity, and for 180 min after KA. At least one 30-min recording similar to baseline was required before ending the experiment.

Ictal episodes are characterized by high-frequency (7-10 Hz) and/or multispike complexes and/or high-voltage (700 μV-1.0 mV) synchronized spikes occurring simultaneously in the injected and contralateral hippocampi. Seizure activity was quantified by measuring the number and total duration of seizures (summing up the duration of each ictal episode during the EEG recording). Seizures occurred with an average latency of about 10 minutes from KA injection, then recurred for about 120 min, and were associated with motor arrest of the mice.

Results

Tg(CJD) mice show an inversion of synaptic metaplasticity associated with alterations in NMDAR composition. The Tg(CJD) mice we used express mutant PrP at a level similar to that of endogenous PrP in WT mice, on a PrP KO genetic background (C57BL/6J/*Prnp*$^{0/0}$); therefore they express transgenic but not endogenous WT PrP (Dossena et al., 2008). They develop deficits in spatial working memory between 200 and 300 days of age; progressive motor dysfunction, first detectable in the accelerating Rotarod test between 300 and 350 days; overt clinical signs, such as ataxia, kyphosis and foot clasp reflex, by ~450 days; and die prematurely at ~700 days (Dossena et al., 2008; Senatore et al., 2012).

We examined synaptic NMDA-dependent long-term plasticity at Schaffer collateral-commissural synapses in the CA1 area on *ex vivo* brain slices from presymptomatic ~100-day-old Tg(CJD) mice, non-transgenic PrP KO littermates, and age-matched C57BL/6J (WT) controls. We first examined the ability of CA3-CA1 synapses to undergo long-term potentiation (LTP). Theta burst stimulation (TBS) resulted in robust LTP in all groups of mice (% of baseline, WT 134 ± 6; PrP KO 143 ± 8; Tg(CJD) 144 ± 10; n = 7-9, $p < 0.05$; Figure A).

Pre-activation of various intracellular signaling pathways before the delivery of a plasticity induction protocol can prime hippocampal synapses by modifying NMDAR activity (Blitzer et al., 1998; Lu et al., 1998; Huang et al., 2001). This priming inhibits the subsequent induction of LTP (MacDonald et al., 2006), a process conceptualized as synaptic metaplasticity (Hulme et al., 2013). When we investigated metaplasticity at CA3-CA1 synapses of WT mice, we found that a low-frequency (10 Hz) priming stimulus (LFS) did not change basal neurotransmission ($p > 0.05$), but prevented the LTP after TBS (100 ± 3% of baseline, n = 7, $p > 0.05$; Figure 1B), consistent with previous findings (Balducci et al., 2010). Like in WT mice, LFS priming did not significantly affect basal synaptic responsiveness in Tg(CJD) and PrP KO animals ($p > 0.05$) but failed to inhibit LTP induction in Tg(CJD) (152 ± 11%, n = 9, $p < 0.05$), and to a lesser extent in PrP KO mice (125 ± 6%, n = 10, $p < 0.05$; Figure 1B).

Hippocampal metaplasticity depends on changes in the localization and composition of postsynaptic NMDARs triggered by the priming stimulation (Christie et al., 1995; Gisabella et al., 2003). The inversion of metaplasticity in Tg(CJD) and PrP KO mice raises the possibility that the composition of NMDARs may be constitutively altered in these mice, impairing further changes after priming. To test this, we analyzed NMDAR subunit composition in hippocampal post-synaptic density (PSD)-enriched fractions by immunoblotting. We found no changes in the total levels of GluN2A, GluN2B and GluN1, but a significant increase in phospho-Tyr1472 GluN2B in Tg(CJD) mice (Figure 2), which is the phosphorylated isoform that potentiates NMDA-induced Ca^{2+} influx. The level of phospho-Tyr1472 GluN2B in PrP KO mice was intermediate between that of WT and Tg(CJD) mice (Figure 2C).

These results indicate abnormal hippocampal NMDAR trafficking in the PSD fractions, with an increase in GluN2B synaptic expression in Tg(CJD) and, to a lesser extent, in PrP KO mice. This correlates well with the impairment in synaptic metaplasticity, which is also more evident in Tg(CJD) mice.

Tg(CJD) mice show age-dependent increases in IL-1β levels in the hippocampus. There is evidence that interleukin-1β (IL-1β) promotes Src family kinase (SFK)-mediated Tyr1472 phosphorylation of GluN2B (Viviani et al., 2003), and its brain levels are high in CJD (Sharief et al., 1999; Shi et al., 2013; Llorens et al., 2014). We investigated IL-1β expression in the hippocampus of Tg(CJD) mice at presymptomatic (60 and 120 days), early (240 days) and advanced (> 400 days) symptomatic stages of their illness (Dossena et al., 2008; Senatore et al., 2012). Immunohistochemistry with an anti-glial fibrillary acid protein (GFAP) antibody confirmed the proliferation and hypertrophy of astrocytes previously documented in Tg(CJD) mice (Dossena et al., 2008). Astrocytosis was already observed in the hippocampus of 60-day-old mice, and increased with age (Figure 3A). Staining with the microglial marker CD11b showed marked microglial activation already at 60 days of age (Figure 3B).

IL-1β immunopositive cells were detected in the hippocampus of Tg(CJD), but not WT and PrP KO mice (Figure 4A). There were gradually more of these cells in older Tg(CJD) mice (Figure 4B). Co-immunofluorescent staining of IL-1β with GFAP, CD11b, or the neuronal marker NeuN (not shown), showed that IL-1β was exclusively expressed by astrocytes (Figure 4C). Quantitative RT-PCR showed a significant increase in IL-1β mRNA in the hippocampus of Tg(CJD) mice already at 60 days of age (Figure 4D).

These results indicate proinflammatory changes in the hippocampus of Tg(CJD) mice starting from a presymptomatic stage. This proinflammatory *milieu*, and particularly IL-1β released from activated astrocytes, may promote neuronal GluN2B phosphorylation over the level induced by loss of PrP function in PrP KO mice. This may contribute to enhancing NMDAR activity in the mutant mice (Viviani et al., 2003).

The IL-1 receptor antagonist rescues the defect in hippocampal metaplasticity and the age-dependent increase in LTP in Tg(CJD) mice. IL-1β signaling participates in the regulation of synaptic plasticity in physiological and pathological conditions (Ross et al., 2003; Costello et al., 2011; Vezzani and Viviani, 2015). To investigate whether the age-dependent elevation of IL-1β in Tg(CJD) mice was associated with changes in hippocampal synaptic plasticity, we analyzed LTP and metaplasticity in ~300-day-old mice. TBS resulted in efficient LTP in WT mice (129 ± 5% of baseline, 10 mice, $p < 0.01$; Figure 5A). LTP was significantly reduced in slices from PrP KO mice (106 ± 5%, 13 mice, p > 0.05; Figure 5A), consistent with the age-dependent impairment in LTP previously documented in these mice (Curtis et al., 2003). In contrast, in Tg(CJD) animals TBS triggered a greater LTP than in WT controls (171 ± 12%, 5 mice, p < 0.05; Figure 5A), indicating enhanced synaptic responsiveness.

When we examined synaptic metaplasticity, we found that the priming stimulus efficiently suppressed LTP in slices from WT animals (107 ± 5% of baseline, 7 mice, p > 0.05), but failed to abolish it in Tg(CJD) mice (145 ± 8%, 5 mice, p < 0.01; Figure 5B), similar to what was seen at ∼100 days. In ∼300-day-old PrP KO mice we could not detect any metaplastic phenomena (107 ± 6%, 5 mice, p > 0.05), due to impaired LTP even in the absence of LFS (Figure 5B). Like in ∼100-day-old animals, the priming protocol did not modify the basal synaptic responses *per se* (Figure 5B).

Next we tested whether blocking IL-1β signaling could correct the abnormal plasticity in Tg(CJD) mice. Bath application of anakinra, the human recombinant IL-1 receptor type 1 antagonist (IL-1Ra), on brain slices from Tg(CJD) mice reduced the LTP to a level comparable to that of WT controls (133 ± 6% of baseline, 5 mice, p < 0.05; Figure 5C). IL-1Ra also normalized metaplasticity in the mutant mice (100 ± 7%, 6 mice, p > 0.05), restoring the effectiveness of the priming protocol in preventing the induction of LTP (Figure 5D).

These results indicate that IL-1β contributes to the metaplastic abnormalities and the age-dependent increase in hippocampal synaptic responsiveness in Tg(CJD) mice.

Tg(CJD) mice have enhanced susceptibility to kainate-induced seizures which depends on IL-1β signaling. Since IL-1β, by promoting SFK activation and GluN2B phosphorylation (Viviani et al., 2003), has proconvulsive effects (Balosso et al., 2008; Galic et al., 2008), we tested whether the Tg(CJD) mice were more prone to seizures. Focal-onset acute seizures were induced by unilateral intrahippocampal injection of KA in Tg(CJD), PrP KO and WT mice aged between 210 and 310 days. EEG recordings showed there were more seizures, and longer time in ictal activity in Tg(CJD) than in PrP KO and WT mice (Figure 6A-C). To test the contribution of IL-1β signaling in this seizure susceptibility, we injected Tg(CJD) mice with IL-1Ra (0.5 μg in 0.5 μL, intracerebroventricularly) 10 min before intrahippocampal KA. The number of seizures and time in ictal activity were significantly reduced in Tg(CJD) but not in WT mice (Figure 6D and E).

To exclude that differences in rearing conditions between commercial WT mice and Tg(CJD) and PrP KO mice raised in-house could affect the results, we compared the susceptibility to kainate-induced seizures of C57BL/6J adult male mice purchased from our external provider and exposed to seizures two weeks after arrival in our animal facility, to that of mice of the same strain, age and sex that were born and raised in-house (7 mice/group). We found no significant differences in time to seizure onset, number of seizures and time in seizure between the two groups (WT raised in-house: 10.0 ± 4.0 min; 7.9 ± 2.3; 6.7 ± 2.3 min; WT from Envigo: 8.0 ± 2.6 min; 6.9 ± 3.7; 5.0 ± 1.8 min; mean ± SD).

Discussion

The present study found that Tg(CJD) mice, which express a misfolded mutant PrP, had alterations in hippocampal metaplasticity and an age-related increase in the magnitude of LTP. They also had high levels of phosphorylated GluN2B, indicative of enhanced NMDAR activity, and were intrinsically more susceptible to hippocampal seizures. Subtle alterations in synaptic metaplasticity and a modest increase in GluN2B phosphorylation were also seen in PrP KO mice. However, these mice had an age-dependent decrease in LTP, and no alterations in hippocampal seizure susceptibility. Tg(CJD) mice had proinflammatory changes, with progressive astro- and micro-gliosis, and more IL-1β-positive astrocytes in the hippocampus. Blocking IL-1β signaling rescued the abnormalities in metaplasticity and the age-related increase in LTP, and significantly reduced susceptibility to seizures.

These findings indicate an enhancement of NMDA-dependent synaptic signaling in the Tg(CJD) hippocampus which may result from a combination of loss and gain of function of mutant PrP, and involves neuroinflammation. They suggest that anti-inflammatory drugs that block IL-1β signaling, perhaps in combination with NMDAR antagonists, may help normalize hippocampal synaptic activity, with beneficial effects on the symptomatic expression of disease.

Tg(CJD) and PrP KO mice develop similar and divergent abnormalities in hippocampal synaptic plasticity. In hippocampal slices from ~100-day-old Tg(CJD) mice LTP was normal at the CA3-CA1 synapses but there was an inversion of metaplasticity, with a significant increase in phosphorylation of the NMDAR GluN2B subunit at tyrosine residue 1472. Phosphorylation at this C-terminal regulatory site prevents endocytosis of GluN2B, enhancing its cell surface expression and NMDAR activity (Salter and Kalia, 2004). In the hippocampus, low-frequency (10-Hz) presynaptic stimulation triggers NMDA-dependent metaplastic changes that inhibit the induction of LTP (Zhang et al., 2005). This homeostatic control may serve to prevent LTP from occurring too readily in response to weak stimuli, or to restrain LTP induction after strong stimuli, thus helping maintain synaptic efficacy within a dynamic range permissive for a learning-ready state and memory retention (Abraham, 2008). The GluN2B-type NMDARs mediate maximal increases in intracellular Ca^{2+} in response to low-frequency stimulation, while GluN2A-type receptors activate maximally in response to high-frequency synaptic inputs (Erreger et al., 2005). The hyper-phosphorylation of GluN2B in Tg(CJD) mice may change the biophysical properties of NMDAR, with consequent alterations in post-synaptic Ca^{2+} dynamic and downstream Ca^{2+}-dependent signaling after the 10-Hz priming stimulus. This may lead to inversion of metaplasticity without affecting LTP, and potentially contribute to the memory impairment that develops in these mice (Dossena et al., 2008).

There was a modest increase in phospho-Tyr1472 GluN2B in PrP KO mice. There is evidence that PrP participates in a signaling cascade that activates SFK Fyn and promotes GluN2B phosphorylation (Um et al., 2012), and loss of PrP may result in constitutive activation of this signaling. We have also found that PrP interacts physically with GluN2B (manuscript in preparation), possibly promoting its intracellular transport, or acting as a scaffold protein to target the receptor to specific microdomains of the synaptic membrane (Senatore et al., 2013). GluN2B may be hyperphosphorylated in PrP KO mice as an adaptive response to permit interaction with other proteins that favor its cell surface expression (Maier et al., 2013). The modest increase of phospho-Tyr1472 GluN2B in the hippocampus of PrP KO mice, however, does not appear to have important functional consequences, since metaplasticity is only slightly altered, and mice are not impaired in hippocampus-dependent learning and memory (Dossena et al., 2008; Bouybayoune et al., 2015) (and unpublished data). Other mechanisms should therefore presumably be operative in Tg(CJD) mice that raise GluN2B phosphorylation over the level induced by loss of PrP, leading to hippocampal dysfunction.

We previously reported that PrP deposition in the brains of Tg(CJD) mice was associated with prominent hypertrophy and proliferation of astrocytes in the hippocampus (Dossena et al., 2008). We have now shown that microglia are also activated, and that both micro- and astro-gliosis prefigure the appearance of neurological deficits and increase further during the symptomatic phase of the disease, most likely reflecting the progressive accumulation of misfolded PrP (Bouybayoune et al., 2015). The novel information is that hippocampal IL-1β is specifically raised in astrocytes, in accordance with previous evidence of high whole-tissue levels in variant and sporadic CJD and in CJD-infected mice (Kordek et al., 1996; Sharief et al., 1999; Shi et al., 2013; Llorens et al., 2014).

The mechanism by which misfolded mutant PrP triggers IL-1β biosynthesis in astroglial cells *in vivo* is not known. Application of the neurotoxic PrP106-126 peptide to cultured astrocytes and microglial cells stimulates their proliferation and IL-1β release through the activation of NF-kB (Forloni et al., 1994; Hafiz and Brown, 2000; Lu et al., 2012), suggesting that the misfolded PrP in the brains of Tg(CJD) mice may have a similar effect.

Electrophysiological analysis detected a dramatic increase in hippocampal LTP magnitude in ~300-day-old Tg(CJD) mice, and weakened LTP in PrP KO littermates, clearly differentiating the effects of mutant PrP from those of PrP deletion. At this age, we saw a marked increase of IL-1β-positive astrocytes in the Tg(CJD) hippocampus. IL-1β dose-dependently induced GluN2B phosphorylation in cultured hippocampal neurons through activation of SFK, and this effect was abolished by the IL-1 receptor antagonist (Viviani et al., 2003). Consistent with a role of IL-1β in altering NMDAR responses in Tg(CJD) mice, IL-1Ra restored normal LTP and rescued the metaplastic defect in brain slices.

Hypersynchronous hippocampal bursting caused by enhanced NMDAR-mediated excitation has been reported in mice infected with vCJD prions (Ratte et al., 2008). In the light of the high IL-1β levels in vCJD patients (Sharief et al., 1999), it may be worth measuring this cytokine in the brain of vCJD-infected mice and test whether anakinra prevents these hypersynchronous hippocampal bursting.

LTP was significantly impaired in ~300-day-old PrP KO mice. An age-related alteration in hippocampal LTP was previously reported in Zürich I PrP KO mice (the strain also used in our study), and in an independently generated line of co-isogenic 129/Ola mice in which the *Prnp* locus was disrupted using a different strategy (Curtis et al., 2003). However, analysis of hippocampal synaptic plasticity in PrP KO mice has produced conflicting results (Collinge et al., 1994; Manson et al., 1995; Lledo et al., 1996; Maglio et al., 2004, 2006). Differences in the induction protocol, animal model and/or age of the mice may account for these. Zürich I mice, as well as mice in which PrP was postnatally ablated only in neurons, also had a significant attenuation of after-hyperpolarization potentials (AHPs) in CA1 pyramidal neurons (Colling et al., 1996; Mallucci et al., 2002), supporting a direct role for PrP in hippocampal excitability.

Tg(CJD) but not PrP KO mice show enhanced susceptibility to hippocampal seizures which depends on IL-1β signaling. Tg(CJD) mice were intrinsically more susceptible to hippocampal seizures, suggesting a low seizure threshold. The competitive IL-1R type 1 antagonist IL-1Ra significantly blocked this effect, indicating that it was mediated by the endogenous IL-1β which was increased in Tg(CJD) mouse hippocampus. In full accordance with this, there is evidence that intra-hippocampally injected IL-1β increases kainate seizures – and other types of seizures – in rodents (Vezzani et al., 1999, 2000; Maroso et al., 2011; Iori et al., 2017), and IL-1β pro-ictogenic effects were blocked by IL-1Ra (Vezzani et al., 1999, 2000). Gliosis was attenuated, disease onset was delayed and survival was significantly prolonged in prion-infected mice lacking IL-1R type 1 (Schultz et al., 2004; Tamguney et al., 2008). IL-1β's effects on seizures are mediated by Src family kinase phosphorylation of GluN2B which promotes neuronal Ca^{2+} influx (Viviani et al., 2003;

Balosso et al., 2008). Since IL-1β is increased in the brain and CSF of CJD patients, this may contribute to the synaptic alterations and seizures in patients in the advanced stages of the disease (Wieser et al., 2006). These data support the idea that anakinra, or other anti-IL-1β drugs, might have therapeutic effects in prion diseases.

At variance with previous observations (Walz et al., 1999; Rangel et al., 2007), we found no difference in susceptibility to seizures between PrP KO and WT mice; this might be due to focal rather than systemic administration of KA, the latter also involving extra hippocampal brain regions contributing to seizures. In addition, we used mice with a homogeneous C57BL/6J background, whereas other studies used PrP KO mice with mixed genetic backgrounds (typically 129Sv X C57BL/6J), and genetic heterogeneity may profoundly affect seizure susceptibility in mice (Schauwecker, 2011; Striebel et al., 2013a, 2013b).

Animal husbandry and rearing conditions can also affect susceptibility to seizures (Leussis and Heinrichs, 2006, 2009), and our C57BL/6J controls were purchased from an external provider whereas the Tg(CJD) and PrP KO mice were raised in-house. However, this difference is unlikely to have affected our results since we found no differences in seizure susceptibility between C57BL/6J mice purchased from Envigo and those that were born and raised in-house. Moreover, all mice from the external vendor were housed for at least two weeks in our animal facilities together with Tg(CJD) and PrP KO mice before being used for the experiments.

In summary, we provide evidence of dysfunctional NMDA-dependent hippocampal synaptic plasticity and enhanced seizure susceptibility in Tg(CJD) mice. These effects appear to result from altered NMDAR activity and neuroinflammation. Targeting NMDAR and IL-1β signaling with clinically available drugs may be beneficial in the symptomatic treatment of the disease.

References

Abraham WC (2008) Metaplasticity: tuning synapses and networks for plasticity. Nat Rev Neurosci 9:387.

Balducci C, Tonini R, Zianni E, Nazzaro C, Fiordaliso F, Salio M, Vismara L, Gardoni F, Di Luca M, Carli M, Forloni G (2010) Cognitive deficits associated with alteration of synaptic metaplasticity precede plaque deposition in AbetaPP23 transgenic mice. J Alzheimers Dis 21:1367–1381.

Balosso S, Maroso M, Sanchez-Alavez M, Ravizza T, Frasca A, Bartfai T, Vezzani A (2008) A novel non-transcriptional pathway mediates the proconvulsive effects of interleukin-1beta. Brain 131:3256–3265.

Blitzer RD, Connor JH, Brown GP, Wong T, Shenolikar S, Iyengar R, Landau EM (1998) Gating of CaMKII by cAMP-regulated protein phosphatase activity during LTP. Science 280:1940–1942.

Bouybayoune I et al. (2015) Transgenic fatal familial insomnia mice indicate prion infectivity-independent mechanisms of pathogenesis and phenotypic expression of disease. PLoS Pathog 11:e1004796.

Brown DR, Herms JW, Schmidt B, Kretzschmar HA (1997) Prp and Beta-Amyloid Fragments Activate

Different Neurotoxic Mechanisms In Cultured Mouse Cells. Eur J Neurosci 9:1162–1169.

Bueler H, Fischer M, Lang Y, Bluethmann H, Lipp HP, DeArmond SJ, Prusiner SB, Aguet M, Weissmann C (1992) Normal development and behaviour of mice lacking the neuronal cell-surface PrP protein. Nature 356:577–582.

Carulla P, Llorens F, Matamoros-Angles A, Aguilar-Calvo P, Espinosa JC, Gavin R, Ferrer I, Legname G, Torres JM, del Rio JA (2015) Involvement of PrP(C) in kainate-induced excitotoxicity in several mouse strains. Sci Rep 5:11971.

Chiesa R (2015) The elusive role of the prion protein and the mechanism of toxicity in prion disease. PLoS Pathog 11:e1004745.

Christie BR, Stellwagen D, Abraham WC (1995) Reduction of the threshold for long-term potentiation by prior theta-frequency synaptic activity. Hippocampus 5:52–59.

Colby DW, Prusiner SB (2011) Prions. Cold Spring Harb Perspect Biol 3:a006833.

Colling SB, Collinge J, Jefferys JG (1996) Hippocampal slices from prion protein null mice: disrupted Ca(2+)-activated K+ currents. Neurosci Lett 209:49–52.

Collinge J, Whittington MA, Sidle KC, Smith CJ, Palmer MS, Clarke AR, Jefferys JG (1994) Prion protein is necessary for normal synaptic function. Nature 370:295–297.

Costello DA, Claret M, Al-Qassab H, Plattner F, Irvine EE, Choudhury AI, Giese KP, Withers DJ, Pedarzani P (2012) Brain deletion of insulin receptor substrate 2 disrupts hippocampal synaptic plasticity and metaplasticity. PloS One 7:e31124.

Costello DA, Watson MB, Cowley TR, Murphy N, Murphy Royal C, Garlanda C, Lynch MA (2011) Interleukin-1alpha and HMGB1 mediate hippocampal dysfunction in SIGIRR-deficient mice. J Neurosci 31:3871–3879.

Curtis J, Errington M, Bliss T, Voss K, MacLeod N (2003) Age-dependent loss of PTP and LTP in the hippocampus of PrP-null mice. Neurobiol Dis 13:55–62.

De Simoni MG, Perego C, Ravizza T, Moneta D, Conti M, Marchesi F, De Luigi A, Garattini S, Vezzani A (2000) Inflammatory cytokines and related genes are induced in the rat hippocampus by limbic status epilepticus. Eur J Neurosci 12:2623–2633.

Dossena S et al. (2008) Mutant prion protein expression causes motor and memory deficits and abnormal sleep patterns in a transgenic mouse model. Neuron 60:598–609.

Erreger K, Dravid SM, Banke TG, Wyllie DJA, Traynelis SF (2005) Subunit-specific gating controls rat NR1/NR2A and NR1/NR2B NMDA channel kinetics and synaptic signalling profiles. J Physiol 563:345–358.

Espinosa PS, Bensalem-Owen MK, Fee DB (2010) Sporadic Creutzfeldt-Jakob disease presenting as nonconvulsive status epilepticus case report and review of the literature. Clin Neurol Neurosurg 112:537–540.

Forloni G, Del Bo R, Angeretti N, Chiesa R, Smiroldo S, Doni R, Ghibaudi E, Salmona M, Porro M, Verga L, et al. (1994) A neurotoxic prion protein fragment induces rat astroglial proliferation and hypertrophy. Eur J Neurosci 6:1415–1422.

Galic MA, Riazi K, Heida JG, Mouihate A, Fournier NM, Spencer SJ, Kalynchuk LE, Teskey GC, Pittman QJ (2008) Postnatal inflammation increases seizure susceptibility in adult rats. J Neurosci 28:6904–6913.

Gisabella B, Rowan MJ, Anwyl R (2003) Mechanisms underlying the inhibition of long-term potentiation by preconditioning stimulation in the hippocampus in vitro. Neuroscience 121:297–305.

Hafiz FB, Brown DR (2000) A model for the mechanism of astrogliosis in prion disease. Mol Cell Neurosci 16:221–232.

Head MW, Ironside JW (2012) Review: Creutzfeldt-Jakob disease: prion protein type, disease phenotype and agent strain. Neuropathol Appl Neurobiol 38:296–310.

Huang Y, Lu W, Ali DW, Pelkey KA, Pitcher GM, Lu YM, Aoto H, Roder JC, Sasaki T, Salter MW, MacDonald JF (2001) CAKbeta/Pyk2 kinase is a signaling link for induction of long-term potentiation in CA1 hippocampus. Neuron 29:485–496.

Hulme SR, Jones OD, Abraham WC (2013) Emerging roles of metaplasticity in behaviour and disease. Trends Neurosci 36:353–362.

Iori V, Iyer AM, Ravizza T, Beltrame L, Paracchini L, Marchini S, Cerovic M, Hill C, Ferrari M, Zucchetti M, Molteni M, Rossetti C, Brambilla R, Steve White H, D'Incalci M, Aronica E, Vezzani A (2017) Blockade of the IL-1R1/TLR4 pathway mediates disease-modification therapeutic effects in a model of acquired epilepsy. Neurobiol Dis 99:12–23.

Iori V, Maroso M, Rizzi M, Iyer AM, Vertemara R, Carli M, Agresti A, Antonelli A, Bianchi ME, Aronica E, Ravizza T, Vezzani A (2013) Receptor for Advanced Glycation Endproducts is upregulated in temporal lobe epilepsy and contributes to experimental seizures. Neurobiol Dis 58:102–114.

Khosravani H, Zhang Y, Tsutsui S, Hameed S, Altier C, Hamid J, Chen L, Villemaire M, Ali Z, Jirik FR, Zamponi GW (2008) Prion protein attenuates excitotoxicity by inhibiting NMDA receptors. J Cell Biol 181:551–565.

Kilkenny C, Browne WJ, Cuthill IC, Emerson M, Altman DG (2010) Improving bioscience research reporting: the ARRIVE guidelines for reporting animal research. PLoS Biol 8:e1000412.

Kordek R, Nerurkar VR, Liberski PP, Isaacson S, Yanagihara R, Gajdusek DC (1996) Heightened expression of tumor necrosis factor alpha, interleukin 1 alpha, and glial fibrillary acidic protein in experimental Creutzfeldt-Jakob disease in mice. Proc Natl Acad Sci U A 93:9754–9758.

Leussis MP, Heinrichs SC (2006) Routine tail suspension husbandry facilitates onset of seizure susceptibility in EL mice. Epilepsia 47:801–804.

Leussis MP, Heinrichs SC (2009) Quality of rearing guides expression of behavioral and neural seizure phenotypes in EL mice. Brain Res 1260:84–93.

Lledo PM, Tremblay P, DeArmond SJ, Prusiner SB, Nicoll RA (1996) Mice deficient for prion protein exhibit normal neuronal excitability and synaptic transmission in the hippocampus. Proc Natl Acad Sci U A 93:2403–2407.

Llorens F, Lopez-Gonzalez I, Thune K, Carmona M, Zafar S, Andreoletti O, Zerr I, Ferrer I (2014) Subtype and regional-specific neuroinflammation in sporadic creutzfeldt-jakob disease. Front Aging Neurosci 6:198.

Lu Y, Liu A, Zhou X, Kouadir M, Zhao W, Zhang S, Yin X, Yang L, Zhao D (2012) Prion peptide PrP106-126 induces inducible nitric oxide synthase and proinflammatory cytokine gene expression through the activation of NF-kappaB in macrophage cells. DNA Cell Biol 31:833–838.

Lu YM, Roder JC, Davidow J, Salter MW (1998) Src activation in the induction of long-term potentiation in CA1 hippocampal neurons. Science 279:1363–1367.

MacDonald JF, Jackson MF, Beazely MA (2006) Hippocampal long-term synaptic plasticity and signal amplification of NMDA receptors. Crit Rev Neurobiol 18:71–84.

Maglio LE, Martins VR, Izquierdo I, Ramirez OA (2006) Role of cellular prion protein on LTP expression in aged mice. Brain Res 1097:11–18.

Maglio LE, Perez MF, Martins VR, Brentani RR, Ramirez OA (2004) Hippocampal synaptic plasticity in mice devoid of cellular prion protein. Brain Res Mol Brain Res 131:58–64.

Maier W, Bednorz M, Meister S, Roebroek A, Weggen S, Schmitt U, Pietrzik CU (2013) LRP1 is critical for the surface distribution and internalization of the NR2B NMDA receptor subtype. Mol Neurodegener 8:25.

Mallucci GR, Ratte S, Asante EA, Linehan J, Gowland I, Jefferys JG, Collinge J (2002) Post-natal knockout of prion protein alters hippocampal CA1 properties, but does not result in neurodegeneration. Embo J 21:202–10.

Manson JC, Hope J, Clarke AR, Johnston A, Black C, MacLeod N (1995) PrP gene dosage and long term potentiation. Neurodegeneration 4:113–114.

Maroso M, Balosso S, Ravizza T, Iori V, Wright CI, French J, Vezzani A (2011) Interleukin-1beta biosynthesis inhibition reduces acute seizures and drug resistant chronic epileptic activity in mice. Neurotherapeutics 8:304–315.

Mejías-Aponte CA, Jiménez-Rivera CA, Segarra AC (2002) Sex differences in models of temporal lobe epilepsy: role of testosterone. Brain Res 944:210–218.

Muller WE, Ushijima H, Schroder HC, Forrest JM, Schatton WF, Rytik PG, Heffner-Lauc M (1993) Cytoprotective effect of NMDA receptor antagonists on prion protein (PrionSc)-induced toxicity in rat cortical cell cultures. Eur J Pharmacol 246:261–267.

Nazzaro C, Greco B, Cerovic M, Baxter P, Rubino T, Trusel M, Parolaro D, Tkatch T, Benfenati F, Pedarzani P, Tonini R (2012) SK channel modulation rescues striatal plasticity and control over habit in cannabinoid tolerance. Nat Neurosci 15:284–293.

Perovic S, Pergande G, Ushijima H, Kelve M, Forrest J, Muller WE (1995) Flupirtine partially prevents neuronal injury induced by prion protein fragment and lead acetate. Neurodegeneration 4:369–374.

Puoti G, Bizzi A, Forloni G, Safar JG, Tagliavini F, Gambetti P (2012) Sporadic human prion diseases: molecular insights and diagnosis. Lancet Neurol 11:618–628.

Rangel A, Burgaya F, Gavin R, Soriano E, Aguzzi A, Del Rio JA (2007) Enhanced susceptibility of Prnp-deficient mice to kainate-induced seizures, neuronal apoptosis, and death: Role of AMPA/kainate receptors. J Neurosci Res 85:2741–2755.

Rangel A, Madronal N, Gruart A, Gavin R, Llorens F, Sumoy L, Torres JM, Delgado-Garcia JM, Del Rio JA (2009) Regulation of GABA(A) and glutamate receptor expression, synaptic facilitation and long-term potentiation in the hippocampus of prion mutant mice. PLoS One 4:e7592.

Ratte S, Prescott SA, Collinge J, Jefferys JG (2008) Hippocampal bursts caused by changes in NMDA receptor-dependent excitation in a mouse model of variant CJD. Neurobiol Dis 32:96–104.

Resenberger UK, Harmeier A, Woerner AC, Goodman JL, Muller V, Krishnan R, Vabulas RM, Kretzschmar HA, Lindquist S, Hartl FU, Multhaup G, Winklhofer KF, Tatzelt J (2011) The cellular prion protein mediates neurotoxic signalling of beta-sheet-rich conformers independent of prion replication. EMBO J 30:2057–2070.

Ross FM, Allan SM, Rothwell NJ, Verkhratsky A (2003) A dual role for interleukin-1 in LTP in mouse hippocampal slices. J Neuroimmunol 144:61–67.

Salter MW, Kalia LV (2004) Src kinases: a hub for NMDA receptor regulation. Nat Rev Neurosci 5:317–328.

Schauwecker PE (2011) The relevance of individual genetic background and its role in animal models of epilepsy. Epilepsy Res 97:1–11.

Schultz J, Schwarz A, Neidhold S, Burwinkel M, Riemer C, Simon D, Kopf M, Otto M, Baier M (2004) Role of interleukin-1 in prion disease-associated astrocyte activation. Am J Pathol 165:671–678.

Senatore A, Colleoni S, Verderio C, Restelli E, Morini R, Condliffe SB, Bertani I, Mantovani S, Canovi M, Micotti E, Forloni G, Dolphin AC, Matteoli M, Gobbi M, Chiesa R (2012) Mutant PrP suppresses glutamatergic neurotransmission in cerebellar granule neurons by impairing membrane delivery of VGCC alpha(2)delta-1 subunit. Neuron 74:300–313.

Senatore A, Restelli E, Chiesa R (2013) Synaptic dysfunction in prion diseases: a trafficking problem? Int J Cell Biol 2013:543803.

Sharief MK, Green A, Dick JP, Gawler J, Thompson EJ (1999) Heightened intrathecal release of proinflammatory cytokines in Creutzfeldt-Jakob disease. Neurology 52:1289–1291.

Shi Q, Xie WL, Zhang B, Chen LN, Xu Y, Wang K, Ren K, Zhang XM, Chen C, Zhang J, Dong XP (2013) Brain microglia were activated in sporadic CJD but almost unchanged in fatal familial insomnia and G114V genetic CJD. Virol J 10:216.

Sikorska B, Knight R, Ironside JW, Liberski PP (2012) Creutzfeldt-Jakob disease. Adv Exp Med Biol 724:76–90.

Striebel JF, Race B, Chesebro B (2013a) Prion protein and susceptibility to kainate-induced seizures: genetic pitfalls in the use of PrP knockout mice. Prion 7:280–285.

Striebel JF, Race B, Pathmajeyan M, Rangel A, Chesebro B (2013b) Lack of influence of prion protein gene expression on kainate-induced seizures in mice: studies using congenic, coisogenic and transgenic strains. Neuroscience 238:11–18.

Tamguney G et al. (2008) Genes contributing to prion pathogenesis. J Gen Virol 89:1777–1788.

Thellung S, Gatta E, Pellistri F, Corsaro A, Villa V, Vassalli M, Robello M, Florio T (2012) Excitotoxicity through NMDA receptors mediates cerebellar granule neuron apoptosis induced by prion protein 90-231 fragment. Neurotox Res Available at: http://www.ncbi.nlm.nih.gov/pubmed/22855343.

Trusel M, Cavaccini A, Gritti M, Greco B, Saintot P-P, Nazzaro C, Cerovic M, Morella I, Brambilla R, Tonini R (2015) Coordinated Regulation of Synaptic Plasticity at Striatopallidal and Striatonigral Neurons Orchestrates Motor Control. Cell Rep 13:1353–1365.

Twele F, Töllner K, Brandt C, Löscher W (2016) Significant effects of sex, strain, and anesthesia in the intrahippocampal kainate mouse model of mesial temporal lobe epilepsy. Epilepsy Behav EB 55:47–56.

Um JW, Nygaard HB, Heiss JK, Kostylev MA, Stagi M, Vortmeyer A, Wisniewski T, Gunther EC, Strittmatter SM (2012) Alzheimer amyloid-beta oligomer bound to postsynaptic prion protein activates Fyn to impair neurons. Nat Neurosci 15:1227–1235.

Vezzani A, Conti M, De Luigi A, Ravizza T, Moneta D, Marchesi F, De Simoni MG (1999) Interleukin-1beta immunoreactivity and microglia are enhanced in the rat hippocampus by focal kainate application: functional evidence for enhancement of electrographic seizures. J Neurosci Off J Soc Neurosci 19:5054–5065.

Vezzani A, Moneta D, Conti M, Richichi C, Ravizza T, De Luigi A, De Simoni MG, Sperk G, Andell-Jonsson S, Lundkvist J, Iverfeldt K, Bartfai T (2000) Powerful anticonvulsant action of IL-1 receptor antagonist on intracerebral injection and astrocytic overexpression in mice. Proc Natl Acad Sci U S A 97:11534–11539.

Vezzani A, Viviani B (2015) Neuromodulatory properties of inflammatory cytokines and their impact on neuronal excitability. Neuropharmacology 96:70–82.

Viviani B, Bartesaghi S, Gardoni F, Vezzani A, Behrens MM, Bartfai T, Binaglia M, Corsini E, Di Luca M, Galli CL, Marinovich M (2003) Interleukin-1beta enhances NMDA receptor-mediated intracellular calcium increase through activation of the Src family of kinases. J Neurosci 23:8692–8700.

Walz R, Amaral OB, Rockenbach IC, Roesler R, Izquierdo I, Cavalheiro EA, Martins VR, Brentani RR (1999) Increased sensitivity to seizures in mice lacking cellular prion protein. Epilepsia 40:1679–1682.

Wieser HG, Schindler K, Zumsteg D (2006) EEG in Creutzfeldt-Jakob disease. Clin Neurophysiol 117:935–951.

Zhang L, Kirschstein T, Sommersberg B, Merkens M, Manahan-Vaughan D, Elgersma Y, Beck H (2005) Hippocampal synaptic metaplasticity requires inhibitory autophosphorylation of Ca2+/calmodulin-dependent kinase II. J Neurosci Off J Soc Neurosci 25:7697–7707.

Figure legends

Figure 1. Young adult Tg(CJD) mice have normal hippocampal plasticity but abnormal metaplasticity. (**A**) Theta burst stimulation (TBS) of Schaffer collaterals induces significant long-term potentiation (LTP) of field post-synaptic potentials (fPSP) responses in CA1 of ~100-day-old WT mice (white circles; RM1W, $F_{7,9}$ = 30, p = 0.0003; Tukey's p < 0.05). LTP was similar in age-matched PrP KO (grey circles; RM1W, $F_{8,9}$ = 26, p = 0.0004; Tukey's p < 0.05) and Tg(CJD) mice (green circles; RM1W, $F_{6,9}$ = 18, p = 0.005; Tukey's p < 0.05) (RM2W, $F_{2,21}$ = 0.7, p = 0.7; WT vs. CJD, p > 0.05, Tukey's post hoc test). Insets, superimposed averaged records (5 traces) from WT (left) PrP KO (center) and Tg(CJD) (right) mice before (gray line) and 35-45 min after the TBS stimulation (red line). (**B**) Preceding the TBS with a priming stimulation (2 trains of 10 pulses at 10Hz, spaced 1 second apart) prevented the LTP in WT mice (white circles; RM1W, $F_{6,9}$ = 0.4, p = 0.6) but not in PrP KO (grey circles; RM1W, $F_{9,9}$ = 13, p = 0.003; Tukey's p < 0.05) or Tg(CJD) mice (green circles; RM1W, $F_{8,9}$ = 22, p = 0.001; Tukey's p < 0.05) (RM2W, $F_{2,23}$ = 0.9, p = 0.5; WT vs. KO, p > 0.05; WT vs. CJD, p < 0.001; KO vs. CJD, p < 0.5, Tukey's post hoc test). The priming stimulus did not significantly alter the fPSP slope in Tg(CJD) mice compared to controls (WT: 100 ± 4% of baseline, 7 mice, RM1W, $F_{6,8}$ = 0.5, p = 0.5; PrP KO: 99 ± 2% of baseline, 10 mice, RM1W, $F_{9,8}$ = 0.2, p = 0.7; Tg(CJD): 111 ± 4% of baseline, 9 mice, RM1W, $F_{8,9}$ = 7, p = 0.02; Tukey's p > 0.05) (RM2W, $F_{2,23}$ = 1.0, p = 0.5; WT vs. PrP KO, p > 0.05; WT vs. Tg(CJD), p > 0.05, Tukey's post hoc test). Insets, superimposed averaged records (5 traces) from WT (left) PrP KO (center) and Tg(CJD) (right) mice before the priming stimulus (gray line), 18-26 min after the low-frequency priming stimulus (LFS) (blue line) and 35-45 min after the TBS (red line). (**A**, **B**) Averaged time courses (mean ± SEM) of normalized fPSP slopes. TBS or LFS (in the metaplasticity experiments) were done at the red and the black arrows, respectively. Dashed horizontal lines define baseline responses.

Figure 2. Increased phospho-Tyr GluN2B in hippocampal post-synaptic fractions of Tg(CJD) and PrP KO mice. (**A**) Triton X-100 insoluble fractions representing the post-synaptic density were isolated from the hippocampi of WT, KO and Tg(CJD) mice. Samples corresponding to 10 μg of protein were analyzed by Western blot with the antibodies indicated. (**B**) The protein levels were quantified by densitometric analysis of Western blots, normalized for the level of actin and expressed as percentages of the level in WT mice. (**C**) Tyrosin 1472-phosphorylated GluN2B was normalized on total GluN2B, and expressed as percentages of the level in WT mice. Data are the mean ± SEM of 8-10 animals at 65-80 days of age; $F_{2,86}$ = 6.541 p = 0.0023 by one-way ANOVA; **p < 0.01 vs. WT by Tukey's post hoc test.

Figure 3. Tg(CJD) mice have proliferation of astrocytes and microglia in the hippocampus. (**A**) Brain sections from Tg(CJD) mice at the ages indicated were stained with anti-glial fibrillar acidic protein (GFAP) antibody. Immunostaining revealed marked astrocytosis in the hippocampus. (**B**) Immunostaining with anti-CD11b shows marked microgliosis in the hippocampus of a Tg(CJD) mouse at 60 days of age compared to an age-matched WT control. Scale bars: 100 μm.CA1, field CA1 of hippocampus;h, hilus of the dentate gyrus.Insets: high magnification of resting (WT) and activated (CJD) microglia.

Figure 4. Tg(CJD) mice have an age-related increase in IL-1β-positive astrocytes in the hippocampus. (**A**) Brain sections from the Tg(CJD), WT and PrP KO mice of the ages indicated were immunostained with anti-IL-1β antibody and nickel-intensified diaminobenzidine. Scale bar: 100 μm. Inset: high magnification of IL-1β-positive cells. (**B**) The IL-1β-immunopositive cells in the hippocampus of the mice of different genotypes and ages were counted and expressed as the -fold change over the numbers in WT mice. Data are mean ± SEM of 4-6 animals (2-3 brain sections each); $F_{4,18} = 22.20$ $p < 0.0001$ by one-way ANOVA; ***p < 0.001; ****p < 0.0001 vs. WT and KO by Tukey's post hoc test. **(C)** Immunofluorescence staining of IL-1β (*red*) and glial fibrillary acidic protein (GFAP) or CD11b (*green*) in the dentate gyrus of the hippocampus of a Tg(CJD) mouse at 72 days of age. Sections were reacted with Hoechst 33258 to stain the cell nuclei (blue). The merged images show co-localization of IL-1β with GFAP, but not with CD11b. Scale bar: 10 μm. **(D)** Total RNA was extracted from the hippocampi of 60-66 day-old WT, PrP KO and Tg(CJD) mice, and analyzed by RT-qPCR for IL-1β and GAPDH. mRNAs were quantified by the ΔΔCt method and expressed as the -fold increase over WT. Data are the mean ± SEM of 4-5 animals per group; $F_{2,17} = 4.506$ $p = 0.0269$ by one-way ANOVA; *p < 0.05 vs. WT and KO by Holm-Sidak's post hoc test.

Figure 5. Aged Tg(CJD) mice have altered hippocampal plasticity and metaplasticity, which are normalized by IL-1 receptor antagonism. (**A**) Theta burst stimulation (TBS) induces LTP at the CA3-CA1 synapses of ~300-days-old WT mice (gray circles; RM1W, $F_{9,9} = 36$, $p < 0.0001$; Tukey's $p < 0.01$). The same protocol fails to induce LTP in brain slices of age-matched PrP KO mice (dark grey circles; RM1W, $F_{12,9} = 1.6$, $p = 0.2$). In slices from Tg(CJD) mice, TBS results in LTP (light green circles; RM1W, $F_{4,9} = 31$, $p = 0.003$; Tukey's $p < 0.05$) larger than in controls (RM2W, $F_{2,25} = 0.9$, $p = 0.6$; WT vs. KO, $p < 0.05$, WT vs. CJD, $p < 0.001$; KO vs. CJD, $p < 0.001$; Tukey's post hoc test). Insets: superimposed averaged records (5 traces) from WT (left) PrP KO (center) and Tg(CJD) (right) mice before (gray line) and 35-45 min after the

TBS (red line). (**B**) Upon LFS priming, LTP was absent in WT mice (gray circles; RM1W, $F_{6,9} = 3$, $p = 0.1$) and PrP KO mice (dark grey circles; RM1W, $F_{4,9} = 1$, $p = 0.4$), but not in Tg(CJD) mice (light green circles; RM1W, $F_{4,9} = 28$, $p = 0.0024$; Tukey's $p < 0.01$) (RM2W, $F_{2,14} = 0.6$, $p = 0.7$; WT vs. KO, $p > 0.05$, WT vs CJD, $p < 0.001$; KO vs. CJD, $p < 0.001$; Tukey's post hoc test). The priming stimulus did not significantly alter fPSP responses in Tg(CJD) mice compared to controls (WT: 92 ± 5% of baseline, 7 mice, RM1W, $F_{6,8} = 1.3$, $p = 0.3$; PrP KO: 98 ± 5% of baseline, 5 mice, RM1W, $F_{4,8}= 0.4$, $p = 0.6$; Tg(CJD): 104 ± 3% of baseline, 5 mice, RM1W, $F_{4,8} = 16$, $p = 0.001$; Tukey's $p > 0.05$) (RM2W, $F_{2,14} = 1.6$, $p = 0.1$; WT vs. KO, $p > 0.05$; WT vs CJD, $p > 0.05$; Tukey's post hoc test). Insets: superimposed averaged records (5 traces) from WT (left) PrP KO (center) and Tg(CJD) (right) mice before the priming stimulus (gray line), 15-25 min after the LFS (blue line), and 35-45 min after the TBS (red line). (A,B) Averaged time courses (mean ± SEM) of normalized fPSP slopes. TBS or LFS (in the metaplasticity experiments) were done at the red and the black arrows, respectively. Dashed horizontal lines define baseline responses. (**C**) Bath application of IL1-Ra reduced the magnitude of LTP in Tg(CJD) mice (brown circles; RM1W, $F_{4,9} = 22$, $p = 0.0055$; Tukey's $p < 0.05$; the green line from panel A is reported here for comparison) to levels comparable to WT mice (black line, reported from panel A for comparison) (RM2W, $F_{2,17} = 0.9$, $p = 0.5$; CJD + IL-1Ra vs. CJD, $p < 0.05$; CJD + IL-1Ra vs. WT, $p > 0.05$; Tukey's post hoc test). Inset, superimposed averaged records (5 traces) from CJD + IL-1Ra before (gray line) and 35-45 min after the TBS (red line). (**D**) Upon bath application of IL-1Ra, the LFS priming protocol prevented LTP in Tg(CJD) mice (brown circles; RM1W, $F_{5,9} = 0.2$, $p = 0.7$; the green line from panel B is reported here for comparison), similarly to WT controls (black line, reported from panel B for comparison) (RM2W, $F_{2,15} = 1.5$, $p = 0.2$; CJD + IL-1Ra vs. CJD, $p < 0.05$; CJD + IL-1Ra vs. WT, $p > 0.05$; Tukey's post hoc test). The priming stimulus did not significantly alter the fPSP responses in CJD mice (94 ± 6% of baseline, 6 mice, RM1W, $F_{5,8} = 1.2$, $p = 0.3$) compared to controls (RM2W, $F_{2,15} = 0.9$, $p = 0.6$; CJD + IL-1Ra vs. CJD, $p > 0.05$; CJD + IL-1Ra vs. WT, $p > 0.05$; Tukey's post hoc test). Inset: superimposed averaged records (5 traces) from CJD + IL-1Ra before the priming stimulus (gray line), 18-26 min after the LFS (blue line) and 35-45 min after the TBS (red line). (C,D) Averaged time courses (mean ± SEM) of normalized fPSP amplitudes. TBS or LFS (in the metaplasticity experiments) were done at the red and the black arrows, respectively. Dashed horizontal lines define baseline responses.

Figure 6. **Tg(CJD) mice have increased susceptibility to kainate-induced seizures, which depends on IL-1β signaling**. (**A**) Representative EEG tracings depicting baseline recordings (top) and ictal activity after intrahippocampal kainic acid (KA) injection (bottom) in the left (LHP) and right (RHP) hippocampus in freely

moving mice. (**B, C**) Number of seizures and time spent in seizures in WT (8), PrP KO (9) and Tg(CJD)(6) mice injected with KA. Data are mean ± SEM; **p<0.01 vs. WT and KO mice by one-way ANOVA ($F_{2,20}$ = 19.41 in B and $F_{2,20}$ = 17.25 in C, p < 0.0001) followed by Tukey's test. (**D, E**) Number of seizures and time spent in seizures in WT and Tg(CJD) mice injected with IL-1Ra (anakinra) or saline (intracerebroventricularly and bilaterally; 0.5 μg in 0.5 μL/side), 10 min before KA. Data are mean ± SEM (9-10 each group); **p < 0.01 vs WT and $^{\#}$p < 0.05 vs. Tg(CJD) + saline by Mann-Whitney test (p = 0.0102 in D and p = 0.0133 in E, Tg(CJD)+IL-1Ra vs Tg(CJD)).

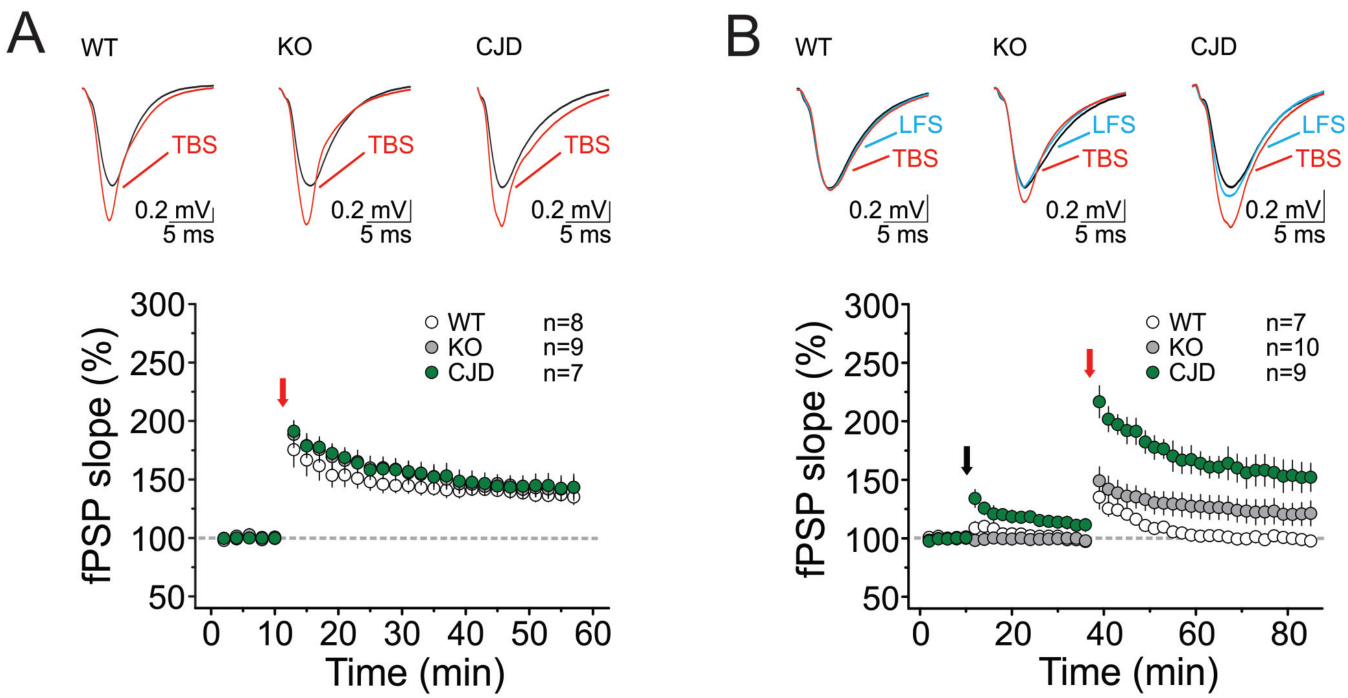
A
WT
KO
CJD
TBS
0.2 mV
5 ms
fPSP slope (%)
Time (min)
WT n=8
KO n=9
CJD n=7
B
LFS
n=7
n=10
n=9

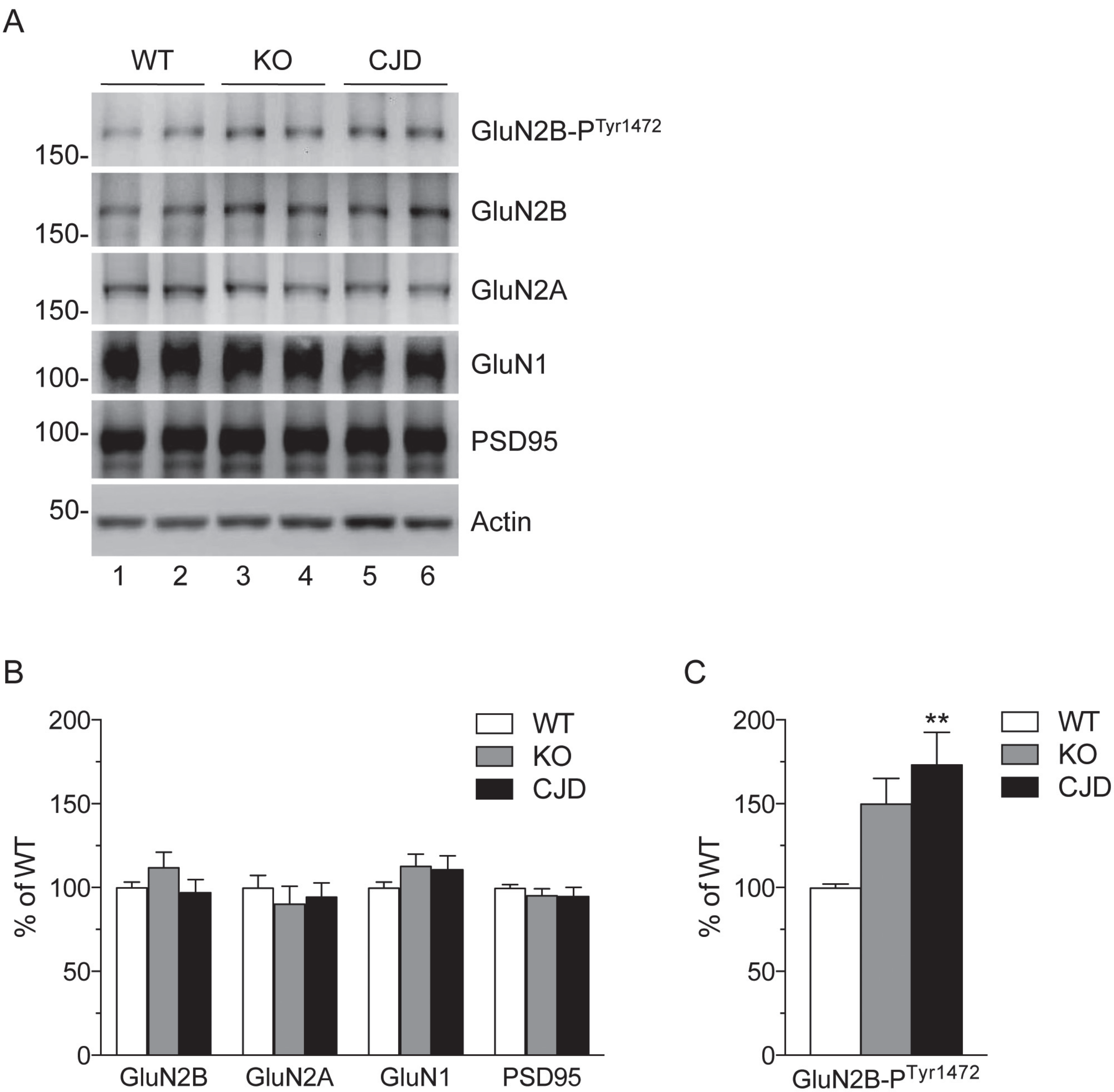
A
WT
KO
CJD
GluN2B-P^Tyr1472
GluN2B
GluN2A
GluN1
PSD95
Actin
150-
150-
150-
100-
100-
50-
1
2
3
4
5
6
B
% of WT
200
150
100
50
0
GluN2B
GluN2A
GluN1
PSD95
WT
KO
CJD
C
% of WT
200
150
100
50
0
**
GluN2B-P^Tyr1472
WT
KO
CJD

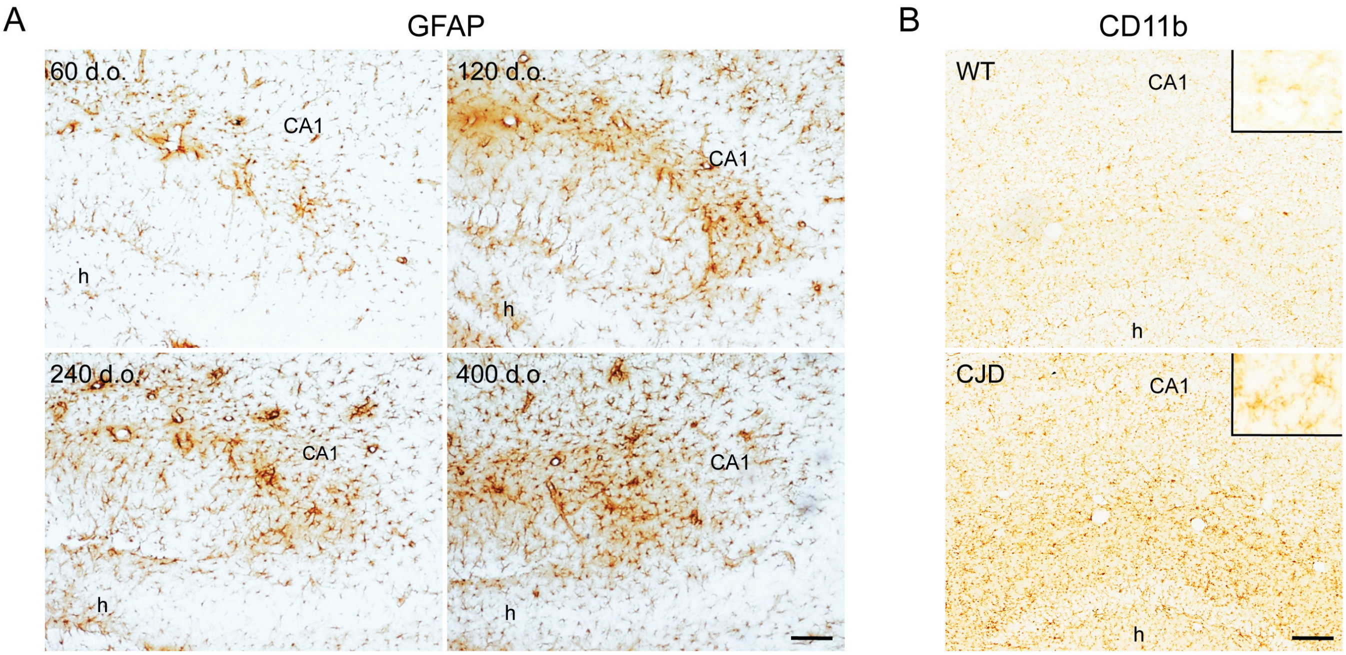
A
GFAP
60 d.o.
CA1
h
120 d.o.
CA1
h
240 d.o.
CA1
h
400 d.o.
CA1
h
B
CD11b
WT
CA1
h
CJD
CA1
h

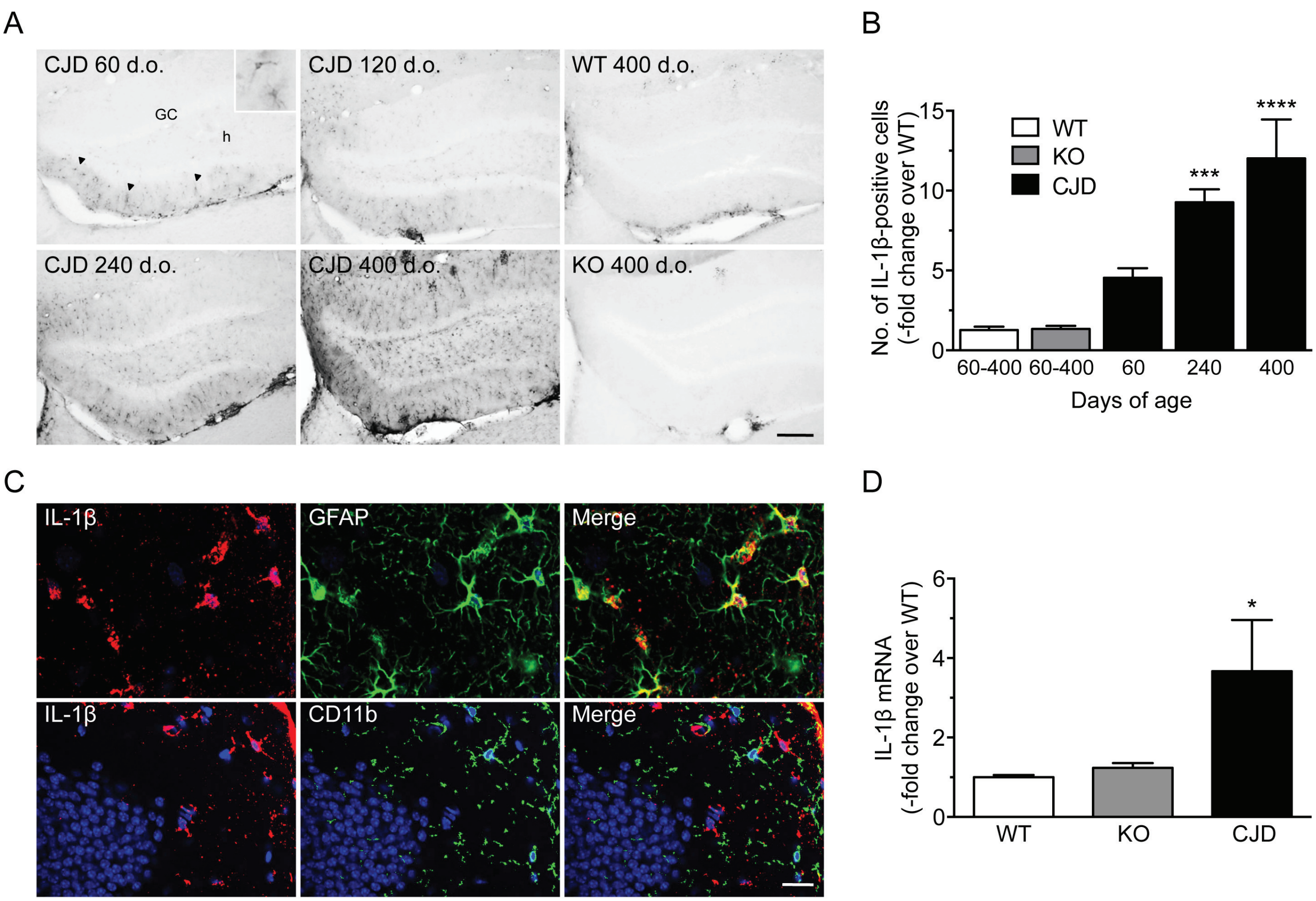
A
CJD 60 d.o.
GC
h
CJD 120 d.o.
WT 400 d.o.
CJD 240 d.o.
CJD 400 d.o.
KO 400 d.o.
B
No. of IL-1β-positive cells
(-fold change over WT)
WT
KO
CJD
***
****
15
10
5
0
60-400
60-400
60
240
400
Days of age
C
IL-1β
GFAP
Merge
IL-1β
CD11b
Merge
D
IL-1β mRNA
(-fold change over WT)
*
6
4
2
0
WT
KO
CJD

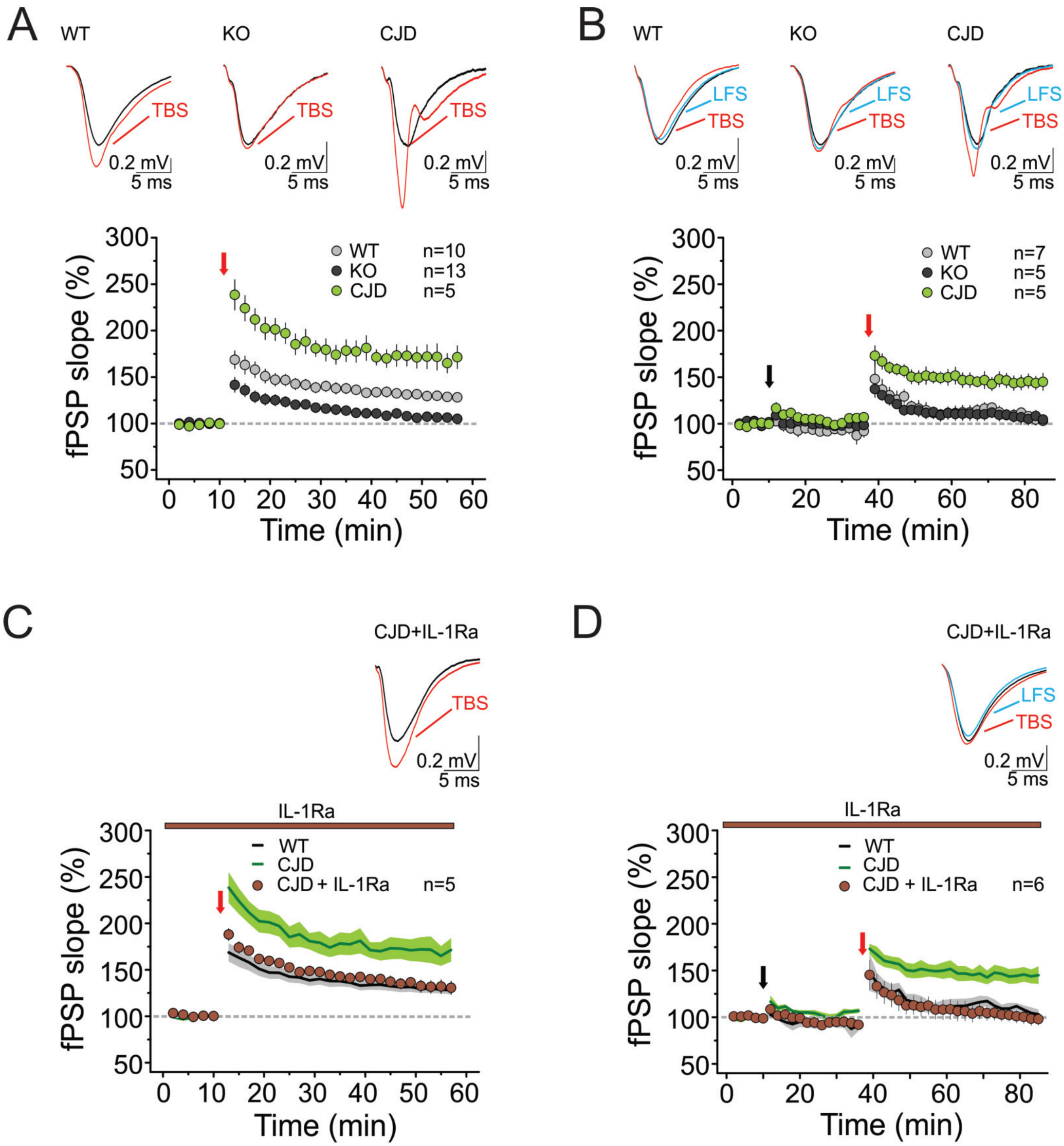

A
WT
KO
CJD
TBS
0.2 mV
5 ms
fPSP slope (%)
Time (min)
WT n=10
KO n=13
CJD n=5
B
LFS
TBS
WT n=7
KO n=5
CJD n=5
C
CJD+IL-1Ra
IL-1Ra
WT
CJD
CJD + IL-1Ra n=5
D
CJD + IL-1Ra n=6

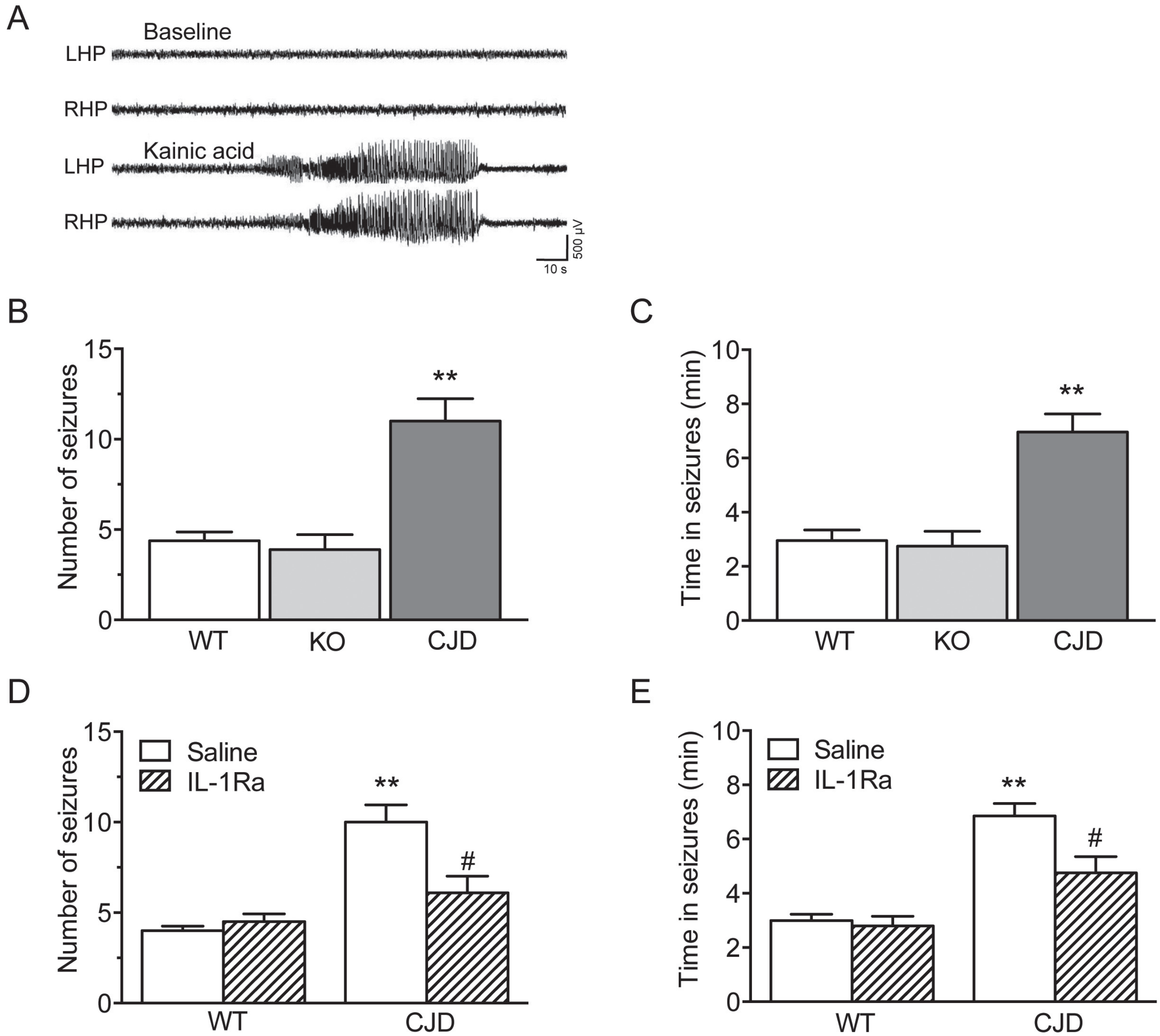
A
Baseline
LHP
RHP
Kainic acid
LHP
RHP
500 µV
10 s
B
Number of seizures
15
10
5
0
**
WT
KO
CJD
C
Time in seizures (min)
10
8
6
4
2
0
**
WT
KO
CJD
D
Number of seizures
Saline
IL-1Ra
**
#
WT
CJD
E
Time in seizures (min)
Saline
IL-1Ra
**
#
WT
CJD